ISSN No:-2456-2165 https://doi.org/10.38124/ijisrt/25dec543

Aerodynamic Characteristics of Uneven Inlet Flow in a Transonic Axial Compressor Operations

Alex Ayedun Avwunuketa[1]

[1]Aeronautical and Astronautical Engineering Department College of Engineering Afe Babalola University Ado -Ekiti Nigeria

Publication Date: 2026/01/06

Abstract: Multi-stage axial compressors are essential component of aerospace propulsion system because the structure of the exit flow field of an axial compressor directly influences the performance and stability of an aerospace engine. In this research paper, the numerical simulations of the first 3 stages of a transonic multi-stage axial compressor were carried out to study the characteristics of the exit flow field of the compressor under four operating conditions. The main focus of the research was airflow deflection angle, patterns of radial velocity distribution, and its changes. Also, the influence of the angle of inlets air direction and pressure on the outlet flow system on the unsteady conditions of inlet airflow were considered. The findings show that when rotational speed reaches a level of 68 %, exit flow field of the axial compressor degrades significantly. The operating conditions, the velocity and airflow angle is positively correlated with the rotational speed as the rotational speed decreases. In comparison to the design condition, the peak velocity reduces by 2%, 3.7% and 7%, whereas airflow deflection angle deviations are less than 3°. Under non-uniform inlet conditions, as the airflow angle at inlet reduced by 90° to 70°, the differences in peak and mean exit velocity do not exceed 2 % and the differences in peak and mean airflow deflection angle do not exceed 1 %. A relatively small effect of alteration in a local pressure field on the inlet pressure in a non-uniform environment produces a very significant impact on the local distributions. When inlet pressure is changed between 1 atm and 1.05 atm, the value of the peak velocity changes by 0.98 percent and that of the average velocity by 3 percent. Maximum difference in velocities is 6 %, and average airflow deflection angle has a difference of 0.7 %, but its maximum deviation valued 1.9°. In general, the characteristics of the flow field on the exit of the compressor demonstrate considerable changes under various operating conditions. The flow in the compressors with low rotational velocities will be more unstable, which causes the flow separation and accumulation of fluid with low energy and non-uniform pressure distribution. On the contrary, variable inlet conditions can have a relatively small impact on the whole flow field, with significant local alterations, which can be used in the theoretical basis to optimized design and performance assessment of compressors.

Keywords: *Aerodynamics, Axial, Compressor, Flow, Transonic.*

How to Cite: Alex Ayedun Avwunuketa (2025) Aerodynamic Characteristics of Uneven Inlet Flow in a Transonic Axial Compressor Operations. *International Journal of Innovative Science and Research Technology*, 10(12), 2453-2461. https://doi.org/10.38124/ijisrt/25dec543

I. INTRODUCTION

The axial-flow compressor is an essential element in the aerospace power system [1]. The data from the compressor outlet help determine the overall functioning of the engine and also forms the initial point for research into the aerodynamic and thermal performance of the combustion chamber, turbine and other parts [2] [3]. It is also the intended flow field for ground tests of the combustion chamber inlet simulation device [4] [5].

When an aero-engine is running, the inlet conditions for the compressor can vary more than predicted [6]. For example, deviation of an inlet can change both the flow speed and direction of the incoming air as it enters the compressor which influences its efficiency and stability [7] [8]. Therefore, studying the compressor outlet flow field with numerical simulations helps achieve better blade design, boost compressor efficiency and enhance the performance of the engine. It is also used as the target flow pattern for inlet simulation at the combustion chamber during ground tests [5].

Furthermore, the inlet conditions for the compressor will not always be the same when the aero-engine is used in practice. For instance, a change in the incoming air velocity and direction by intake distortion [9] [10] [11] can influence how well and effectively the compressor functions. To improve blade design, boost compressor operation and enhance how the engine runs, thorough research of the flow field at the compressor outlet using computer simulations is necessary [12] [13].

ISSN No:-2456-2165 https://doi.org/10.38124/ijisrt/25dec543

Using different techniques, researchers globally have investigated the flow pattern details in a range of pressurized engines. [7] [14] carried out simulations using parallel algorithms on 8.5-stage axial flow pressurized engine in both steady and unsteady conditions. Only a 1–2% error was found when the results were compared to data gathered from experiments. [15] [16] by simulation, created a three-dimensional view of the turbulent flow in the impeller of a multi-stage pressurized axial gasifier. A high-precision, high-resolution third-order ENN method was adopted to reproduce excitement waves and turbulent features and used the LU-SGS implicit solution to improve how quickly the system analyzed the data, to build a dependable and efficient approach for solving turbulent flow issues in a multi-stage transonic axial pressurized gasifier

[17] performed a simulation of the Rotor 37 transonic compressor stage and compared the results to experimental measurements. The rotor 37 was the brainchild of NASA. A part of the NASA Fundamental Aeronautics Program is the assessment of various computational fluid dynamics (CFD) code used by NASA and other industry, to developed and design aircraft, spacecraft and engines types. Rapid convergence and practical usefulness were found to be benefits of using the Runge–Kutta method and finite difference methods. [18] investigated into the application of an 11-stage axial flow compressor by simulating it and its flow field using three-dimensional computer tools. They tested these features at normal operating conditions, different positions and several installation angles. The curves for flow pressure ratio and flow efficiency were compared against experimental results and no errors exceeded the allowed values.

Pressured gas compressor intake, experiences a number of disruptions that result in irregular intake airflow fields [19]. These inlet changes, considerably affect the pressurized air since there is not a steady total pressure and total temperature [20] [21] [22] and a cyclonic flow of the intake air in the system, worsen the aerodynamic performance, stability margins and overall state of the flow [23]. The instability evolution of the compressor under circumferential non-uniform inlet conditions was experimentally examined by [24] [25]. Two kinds of stall inception were studied, each with their own size and starting point, to determine what effects they had on compressor stability. According to [26] [27], uniform pressure at the inlet was used and the temperature variations were converted into pressure variations to find the static pressure at the outlet. [28] did a complete numerical study and laboratory experiment of a transonic pressurized aircraft. [29] did a complete non-stoichiometric investigation of the NASA Rotor 67 engine. Research by [30] performed a numerical study of a transonic fan under complex, time-varying conditions to explore distortion of the final pressure at several distortion degrees and angles. They evaluated and explained the changes in speed, pressure and other system parameters as the total pressure was distorted. [31] explored how high intake pressure distortion impacts the fan booster of a high-bypass-ratio turbofan engine. It was found that an increase in inlet total pressure shifted the outer fan to a position where it faced a risk of surge which lowered its safety margin. With uniform inlet conditions, the total pressure distortion makes the corrected mass flow rate and pressure ratio larger and the corrected mass flow rate changes from 0.2% to 1.0% as the rotational speed is varied from 0.3 to 0.8.

Researchers are focusing their efforts on the areas of aerodynamic performance optimization, surge boundaries predictions, optimizing thermodynamic aspects, adjusting guide vanes and optimizing operation under high-load conditions for axial compressor. The source term method was used by Wang and team [32], to explore inter-stage air injection effects inside a NASA 74A pressurized air compressor, during its first 3.5 stages of operation. The main reason for higher efficiency was found to be an increase in gas flow, caused by decreased inlet angle and avoided flow separation, at the end of the blade. Induced gas created a larger margin of stability in the operating range for the pressurized compressor. [33] and [34] created a way to estimate performance and optimize guide vanes in multi-stage axial-flow compressors using one-dimensional modeling and optimization approaches. The method is proven to accurately predict operation and make the process more efficient which is highly useful for compressor design and control.

Using computational fluid dynamics simulation, the behaviors of the flow at the compressor outlet were studied for the multi-stage axial compressor for different rotational speeds in the first 3 stages. Much attention was given to how airflow deflection angles, radial velocity distributions and their changes were studied. Simulated operating conditions such as design point, climb, cruise, approach and ground idle helped evaluate the effect of rotational speed variations on pressurized air compressor outlet flow. The aim of the findings is to give a theoretical reason for better optimization and performance analysis of pressurized air compressors. The study also looked at how different inlet airflow speeds and angles, as well as pressures, influence the velocity of airflow and the gradients in airflow at the exit.

II. METHODOLOGY

This research considered the first 3 stages which combine the inlet guide vane and the first three actual compressor stages, of the transonic axial-flow compressor. The compressor, which is used for high-pressure and high load testing in experiments on aerodynamics for aero-engines and turbomachinery. The compressor gives information about the characteristics of airflow, flow separation, angles of the airflow and aerodynamic efficiency.

Table 1 lists the key design specifications for the first three stages compressor. The numerical simulations were run in Numeca software (version 16.1) and the compressor was modeled in UG software (version 10.0) based on the 1986 NASA report by [35].

ISSN No:-2456-2165 https://doi.org/10.38124/ijisrt/25dec543

Table 1 Basic Parameters of the First Stage Axial Compressor

Parameter	Value
Rotational speed (rev/min)	16042.3
Tip speed (m/s)	430.29
Number of IGV blade	26
Number of stage 1 rotor blades	28
Number of stage 1 stator blades	34
Number of stage 2 rotor blades	32
Number of stage 2 stator blades	46
Number of stage 3 rotor blades	39
Number of stage 3 stator blades	54
Tip clearance (mm)	0.408

For blade cross-sectioning, the parameters such as chord length, mounting angle, axial placement of key points, blade angle and blade thickness were drawn from the blade structural description. Furthermore, the radial stacking line was defined as the line that connected the locations of maximum thickness along the arcs in the blade pattern. Figures 1 and 2 show the blade model and Figure 3 provides a diagram of the axial compressor.

Fig 1 Diagram Showing Full-Annulus Structure of the Compressor

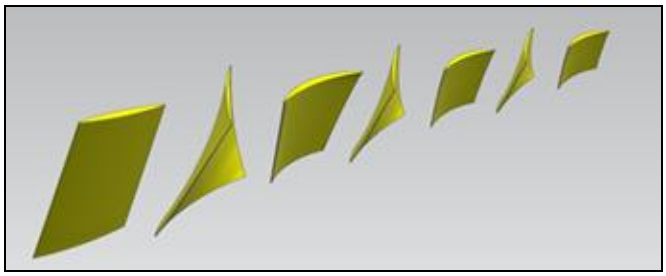

Fig 2 Blade Model of the Compressor.

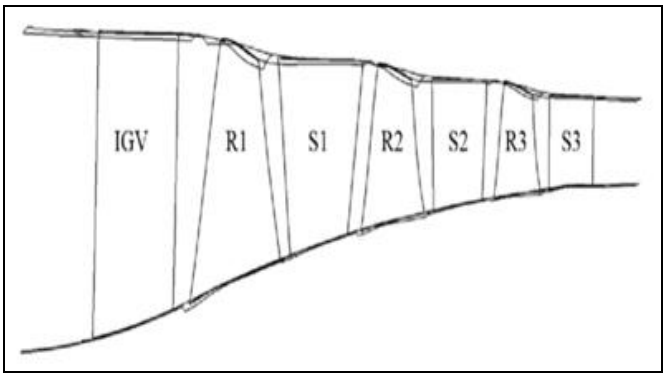

Fig 3 Schematic Diagram of the Meridional Flow Passage of the Compressor [6]

The study investigates how air moves inside an axial compressor which is a gas flow that is viscous and compressible.

The equations that control conservation of mass, momentum and energy in the compressor, take the following forms:

Equation 1 is for conservation of mass.

$$\frac{\delta\rho}{\delta t} + \nabla.(\rho\bar{V}) = 0 \qquad 1$$

Equations 2-4 is for conservation of momentum

$$\frac{\delta}{\delta t}(\rho u) + \nabla.(\rho u V) = -\frac{\delta p}{\delta x} + \frac{\delta}{\delta x}\left[\lambda(\nabla.V) + 2\mu\frac{\delta v}{\delta y}\right] + \frac{\delta\mu}{\delta x}\left[\frac{\delta v}{\delta x} + \frac{\delta u}{\delta y}\right] + \frac{\delta\mu}{\delta z}\left[\frac{\delta u}{\delta z} + \frac{\delta w}{\delta x}\right] \qquad 2$$

$$\frac{\delta}{\delta t}(\rho v) + \nabla.(\rho v V) = -\frac{\delta p}{\delta y} + \frac{\delta}{\delta y}\left[\lambda(\nabla.V) + 2\mu\frac{\delta u}{\delta x}\right] + \frac{\delta\mu}{\delta y}\left[\frac{\delta v}{\delta x} + \frac{\delta u}{\delta y}\right] + \frac{\delta\mu}{\delta z}\left[\frac{\delta w}{\delta y} + \frac{\delta v}{\delta z}\right] \qquad 3$$

$$\frac{\delta}{\delta t}(\rho w) + \nabla.(\rho w V) = -\frac{\delta p}{\delta z} + \frac{\delta}{\delta z}\left[\lambda(\nabla.V) + 2\mu\frac{\delta w}{\delta z}\right] + \frac{\delta\mu}{\delta x}\left[\frac{\delta u}{\delta z} + \frac{\delta w}{\delta x}\right] + \frac{\delta\mu}{\delta y}\left[\frac{\delta w}{\delta y} + \frac{\delta v}{\delta z}\right] \qquad 4$$

Where μ is the dynamic viscosity

Equations 2-4 is also called Navier-stokes equation

Equation (5) is energy equation

$$\frac{\delta}{\delta t}\left[\rho\left(e + \frac{v^2}{2}\right)V\right] + \nabla\left[\rho\left(e + \frac{v^2}{2}\right)V\right] = \rho q - k\nabla^2 T - \nabla.(PV) \qquad \textbf{(5)}$$

Equation (6) is for a compressible flow; the governing equations is.

$$P = \rho RT \qquad \textbf{(6)}$$

The flow field computation was carried out with the help of TURBO solver which is designed by NUMECA. The fluid is assumed to be an ideal air and the computation is a steady-state, single-passage computation using the Reynolds-averaged Navier-stokes (RANS) method. This makes it especially suitable to wall-confined applications of flow simulations for compressor, with accuracy in modelling the

ISSN No:-2456-2165 https://doi.org/10.38124/ijisrt/25dec543

local boundary layer behavior without loss of computational efficiency. At design conditions, the total inlet pressure was to be 101,325 Pa and the total inlet temperature was 288.2 K to align with ISA condition at sea level. The outlet average static pressure is a set value and through changes in outlet static pressure, the compressor characteristic curve is yielded. Moreover, when the rotational speed, as well as the outlet static pressure is set, characteristic curves of various rotational speed conditions are obtained

The generation of the grid was carried out with the help of AutoGrid pre-processing module which is developed by NUMECA, having an H-O-H structure. The inlet and outlet parts used an H-grid, whereas the blade surrounding area was realized with O-structured grid, and mesh refinement in the proximity of the wall surfaces. Radial grid nodes in the gap were set to 17 and the cell was set at 0.003 mm. Figure 4 shows the compressor meridional plane, single-passage and full-annulus grids.

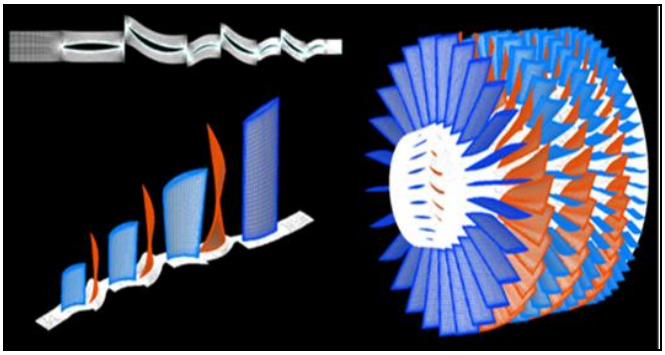

Fig 4 Schematic Diagram of the Meridional Plane, Single Passage and Full-Annulus Mesh Rotor Blades.

In order to achieve part independence of the grid, three meshes that had 3 million, 4.5 million and 6 million mesh elements were used with the results of the computation carried out shown in Figure 5 and 6

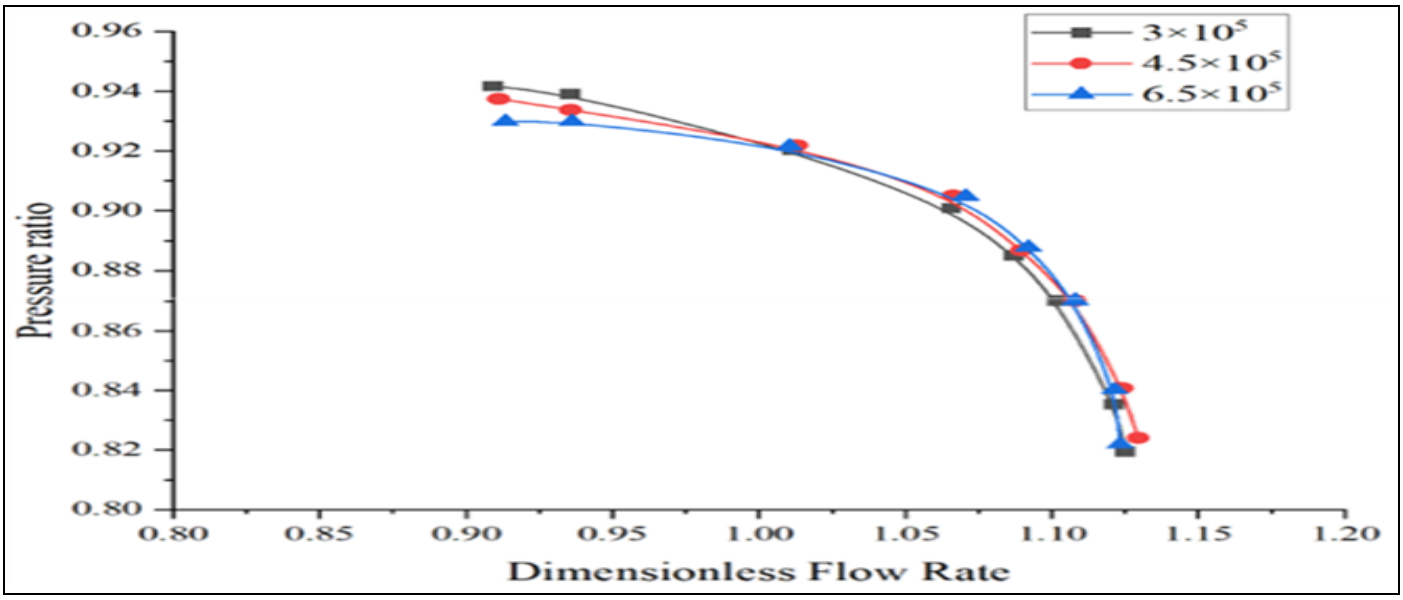

Fig 5 Grid Independence Validation of Pressure Ratio–Mass Flow.

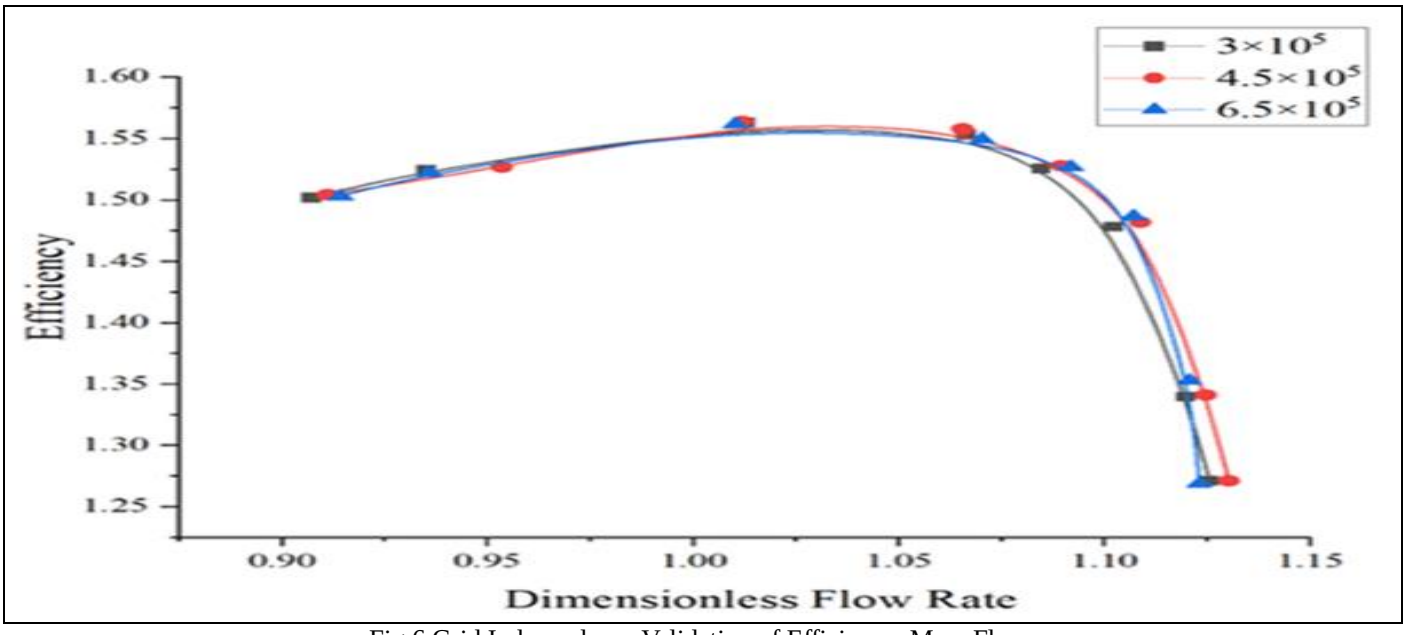

Fig 6 Grid Independence Validation of Efficiency–Mass Flow.

ISSN No:-2456-2165 https://doi.org/10.38124/ijisrt/25dec543

As was seen in the plots, the computed compressor characteristics showed a very small sensitivity to the grids across the various grid resolutions. On the basis of accuracy and computational cost, the grid containing 4.5 million elements was chosen upon which numerical simulation was done. Figure 7 indicates the distribution of the y + values of the grid. Such a grid arrangement provided each orthogonal angle greater than 20 degrees, aspect ratio as well as expansion ratio not to exceed 5000 and 5 respectively, which satisfied the needs of computation.

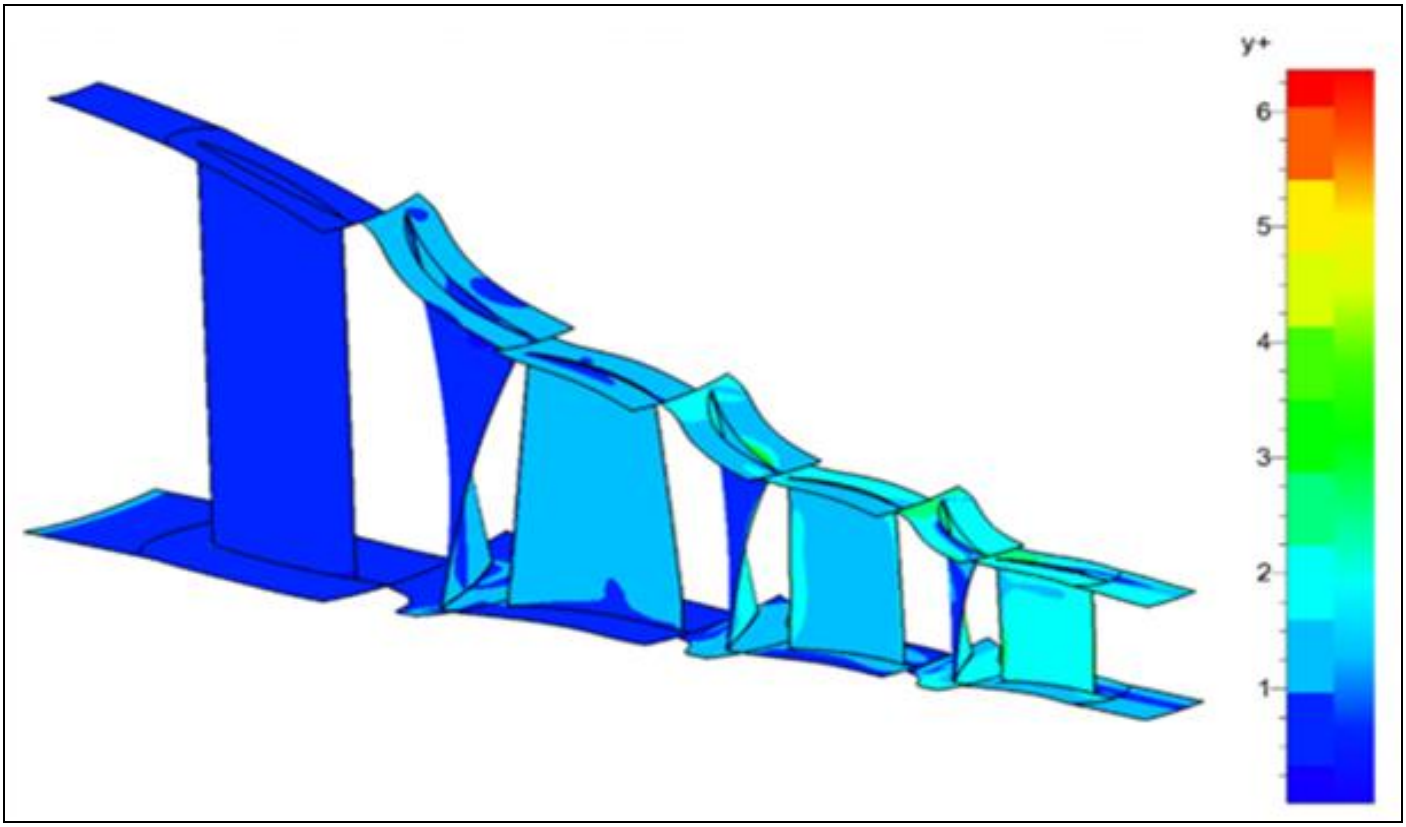

Fig 7 Distribution of Grid y^+ Values.

III. RESULT AND DISCUSSION

This research used five standard compressor operating conditions, to simulate and analyses aircraft engine design speed, at take-off design point of 100%, climb 94%, cruise 93%, approach 89%, and ground idle 68%. These conditions cover most representative points throughout the operation envelope. The research concentrated on the effects of these conditions on compressor exit flow field, in terms of the angles of deflection of airflow entering the compressor and the radial maximum flow and position of the inlet airflow relative to the inlet.

The numerical technique described above was used to simulate the compressor at five different rotational speeds of 100%, 94%, 93%, 89% and 68%. These operating conditions corresponded to rotational speed of 16,042 rpm, 15,079.5 rpm, 14,919 rpm, 14,277.4 rpm and 10,716 rpm, respectively. The compressor mass flow rate was varied, at any given rotational speed, through adjustment of the outlet back pressure. As the backpressure decreases, the compressor mass flow rate, gradually increases. The speed when no additional decrease in backpressure could be applied to yield an increased mass flow rate was then chosen as the choke point of that speed. This is an agreement to work done by [36]. On other hand, increasing backpressure until that brought numerical calculations in a divergence, near-stall point for that speed was identified using the last convergent solution. There is a peak efficiency point on both the mass flow efficiency characteristic curves. The efficiency will fall rapidly to the right of this peak, due to a high flow rate of masses as compared to left, the decline in efficiency is gradual.

Figure 8 and 9 show that the characteristic curves representing the first four rotational speeds of 100%, 94%, 93% and 89% are relatively close to each other with choke flow rates and peak efficiency points being dispersed in a range of about 30-32 kg/s with a very minimal variation.

ISSN No:-2456-2165 https://doi.org/10.38124/ijisrt/25dec543

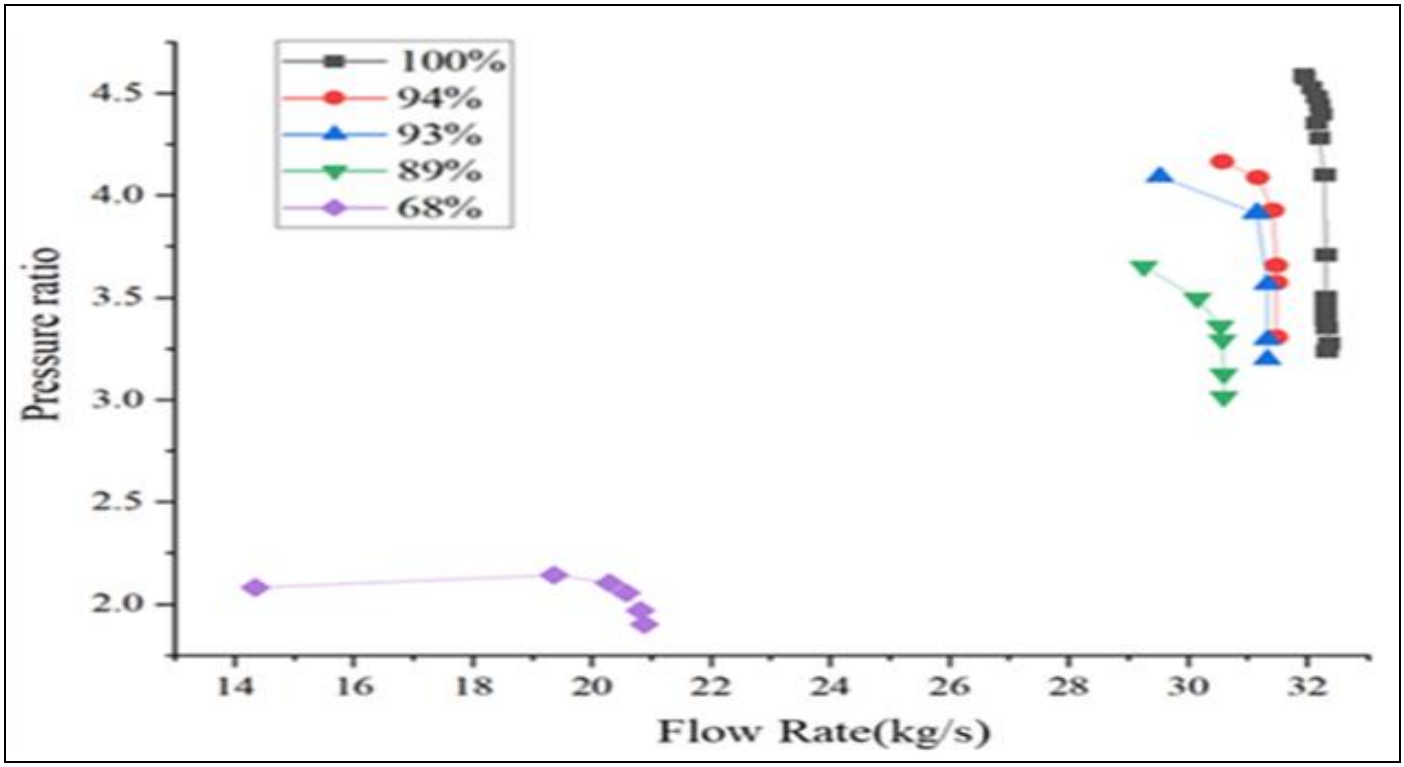

Fig 8 Characteristic Curves of Pressure Ratio-Mass Flow at Different Operating Conditions.

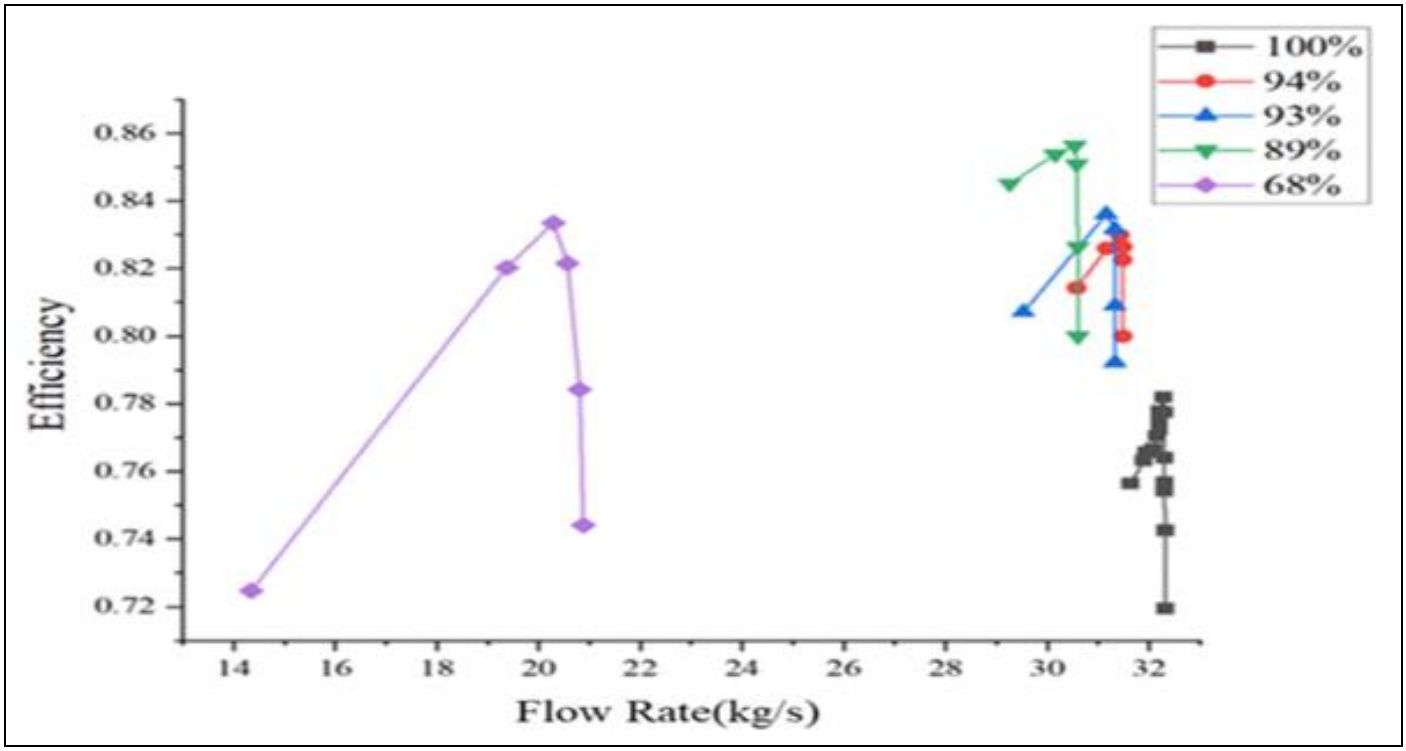

Fig 9 Efficiency-Mass Flow Characteristic Curves at Different Operating Conditions.

Conversely, at 68%, the pressure ratio-mass flow trace has diverged to a great extent, with a mass flow distribution of about 20 kg/s, some 35% lower than at the first four states, showing that we are way off the design operating point.

Figure 10 shows the radial-averaged total velocity distribution curves along blade height at the compressor exit condition under various operating conditions of 100%, 94%, 93%, 89% and 68% of rotational speed.

ISSN No:-2456-2165 https://doi.org/10.38124/ijisrt/25dec543

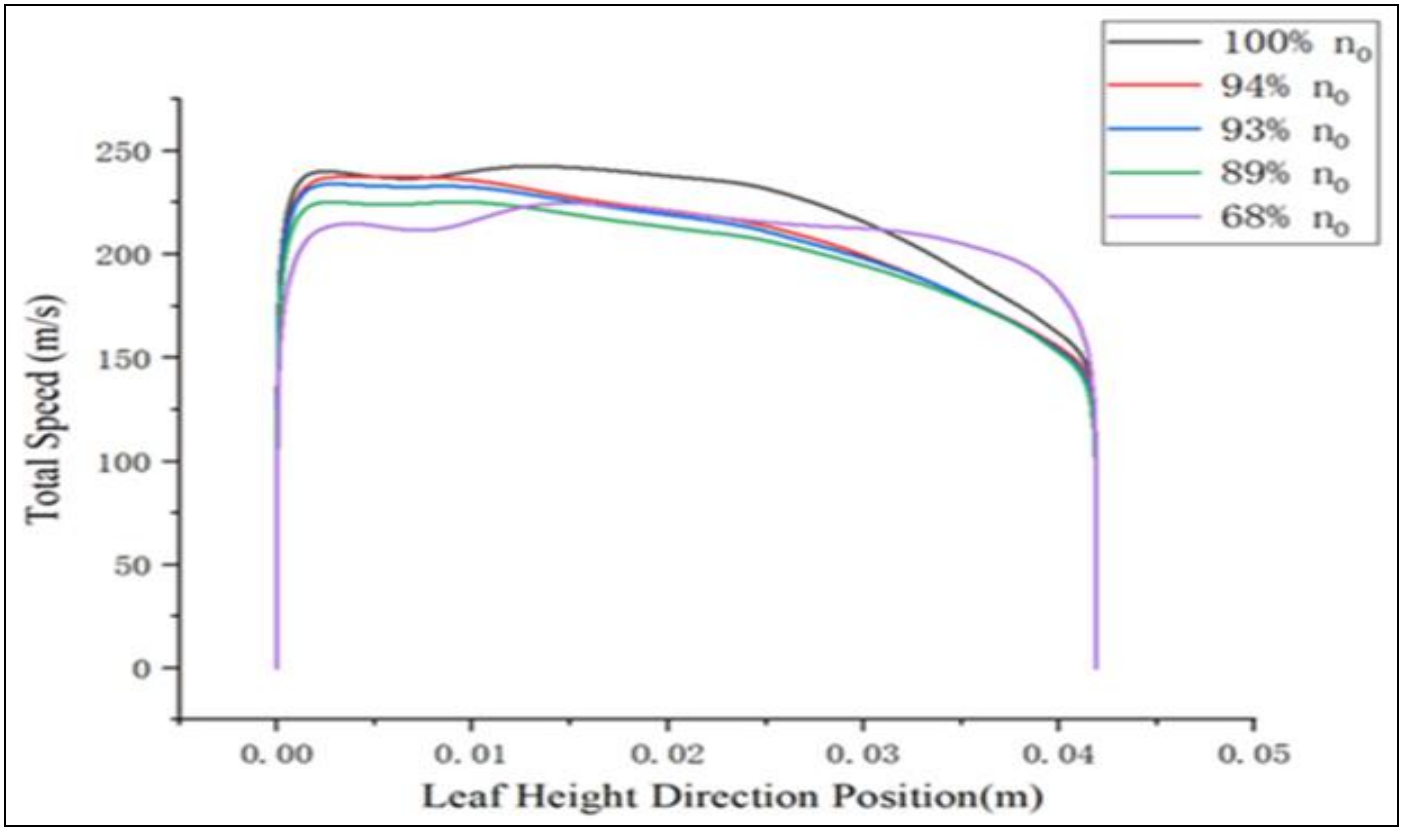

Fig 10 A Comparative of the Mean Total Velocity Distributions along the Radial Direction in the Various Operating Conditions.

By conducting a comparative analysis, one can state that the impact of rotational speed variation on the exit velocity distribution is mainly expressed in the shift of higher velocity and of the shape of the distribution.

The curve of the velocity distribution achieves its maximum total values at the design speed of 100%, and the maximum velocity is about 242.0 m/s. Velocity peak appears approximately in the center of the blade height, and a sharp decrease in velocity is determined between 0.03 m -0.04 m.

The average velocity of100 percent is 219.44 m/s resulting in a higher value than average velocities of the four lower-speed conditions of 208.65 m/s at 94 percent, 206.3 m/s at 93 percent, 201.3 m/s at 89 percent, and 210.3 m/s at 68 percent. This shows that it has higher efficiency in the usage of airflow kinetic energy at the design speed. Also, the average velocity of all the other cases except the 68% condition systematically reduces as the rotational speed decreases.

IV. CONCLUSION

This paper examined the flow field features at the outflow of the initial 3.5 stages of NASA 74A transonic multi-stage axial compressor using numerical method under different rotational speeds. The main aspect analyzed was the airflow deflection angle, radial velocity distribution and the trend in flow variation. With the help of a comparison of real operating conditions to numerical simulation results, it is possible to come to the following conclusions.

With a reduction in the rotational speed of the compressor, the peak and mean exit velocity drop, gradually reducing the stability of the flow field and its overall performance. The maximum velocity at the exit of the compressor is observed at the condition (100 percent n0) as 242.7 m/s and the velocity at the average is 219.44 m/s, which shows promising use of kinetic energy and stable flow field structure. As the rotational speed reduces to 94% n0, 93% n0 and 89% n0, the highest exit velocity tends to reduce gradually to 237.6 m/s, 233.6 m/s and 225.5 m/s respectively with an average of exit velocity in each case to 208.65 m/s, 206.31 m/s and 201.28 m/s respectively. Reductions in peak velocities of 2 percent, 3.7 percent and 7 percent imply reducing flow field stability and compressor performance. The maximum exit velocity at the lowest rotational speed of 68%, n 0, decreases drastically to 220 m/s, which is 11.4 percent off design condition. The velocity distribution gets non-uniform, and the flow separation and low-energy fluid accumulation become very strong, resulting in a massive drop in the overall performance.

The impact of the change in the compressor rotational speed on the exit airflow deflection angle is rather small. In the design conditions (100 % n0), the airflow deflection angle is very confined in the range 85-90 with a maximum swing of 3 leaving the flow field rather homogenous and fairly stable to variation in the rotational speed. But with reduction in the rotational speed, there is a gradual increase in the variation in deflection angle. At 68 percent speed of rotation, the angle of deflection range increases dramatically, and the low-speed region extends. The direction of the airstream guidance becomes much weaker and it is presumed that there is flow instability and more energy is wasted.

ISSN No:-2456-2165 https://doi.org/10.38124/ijisrt/25dec543

Variations in the inlet pressure affect considerably in the distribution of the local flow field but exert a comparatively minor influence in the total flow structure. As the inlet pressure goes up by 5 percent from 1atm to 1.05 atm, mass flow rate and the kinetic energy also increases resulting in an increase in the velocity in the mid-blade area. The maximum difference between the velocity is 0.98% and the average of velocity differences is 3%. At the most difference point, the variation in velocity is 6%. The mean deflection angle of the airflow varies within 0.7% with the largest deviation of 1.9°. All these findings suggest that the change in inlet pressure has a strong impact on local velocity and airflow deflection angle, though its impact on the total flow field distribution is comparatively insignificant.

REFERENCES

[1]. B.Semlitsch, "Boundary conditions to represent the wave impedance characteristics of axial compressors.," *Applied Acoustics*, vol. 4, no. 109236, 2023.

[2]. X. Wang and C. Gu, "Rotor optimization design of a multistage transonic compressor based on entropy loss breakdown analysis," *Aerospace Science and Technology*, vol. 163, no. 110288, 2025.

[3]. J. Jiang, B. Liu, Y. Wang and X. Nan, " Numerical Simulation to Three-Dimensional Turbulent Flow in Multistage Axial Compressor Blade Row," *Journal of Applied Mechanical*, vol. 2, p. 21–25+170, 2007.

[4]. A. Liu, Y. Ju and Z. C. , "Parallel rotor/stator interaction methods and steady/unsteady flow simulations of multi-row axial compressors," *Aerospace Science and Technology*, vol. 116, no. 106859, 2021.

[5]. C. Silva, I. Durán, F. Nicoud and S. Moreau, "Boundary Conditions for the Computation of Thermoacoustic Modes in Combustion Chambers," *AAIA Journal*, vol. 52, no. 6, p. 1180–1193, 2014.

[6]. J. Cheng, J. CHen and H. Xiang, "A surface parametric control and global optimization method for axial flow compressor blades," *Chinese Journal of Aeronautics*, vol. 32, no. 7, pp. 1618-1634, 2019.

[7]. A. Liu, Y. Ju, C. Zhang and R. Dia, "Parallel steady/unsteady flow simulations of an 8.5-stage axial compressor," *Aerospace Science and Technology*, vol. 145, no. 108853, 2024.

[8]. N. Lamarque and T. Poinsot, " Boundary Conditions for Acoustic Eigenmodes Computation in Gas turbine Combustion Chambers," *AIAA Journal*, vol. 46, p. 2282–2292., 2008.

[9]. Y. Sun, "The Influence of Inlet Distortion on the Operating Characteristics of Transonic Axial-Flow Compressor.," Harbin Engineering University, Master's Thesis, Harbin, China,, 2020.

[10]. L. Zhang, Y. Liu and S. Sun, " Numerical study on the effects of different total temperature inlet distortions on the aerodynamic performance and stability of the centrifugal compressor," *Aerospace Science and Technology*, vol. 163, no. 110292, 2025.

[11]. W. Zhang, S. Stapelfeldt and M. Vahdati, "Influence of the inlet distortion on fan stall margin at different rotational speeds," *Aerospace Science and Technology*, vol. 98, no. 105668, 2020.

[12]. W. Gong, G. Liu, J. Wang, F. Wang, A. Lin and Z. Wang, "Aerodynamic and thermodynamic analysis of an aero-engine pre-swirl system based on structure design and performance improvement," *Aerospace Science and Technology*, vol. 23, no. 107466, p. 123, 2022.

[13]. G. Liu, X. Wang, W. Gong and A. Lin, "Prediction of the sealing flow effect on the temperature drop characteristics of a pre-swirl system in an aero-engine," *Applied Thermal Engineering*, vol. 189, no. 1167172021, 2021.

[14]. A. Liu, Y. Ju and C. Zhang, "Parallel rotor/stator interaction methods and steady/unsteady flow simulations of multi-row axial compressors," *Aerospace Science and Technology*, vol. 116, no. 106859, 2021.

[15]. J. Jiang, B. Liu, Y. Wang and X. Nan, " Numerical Simulation to Three-Dimensional Turbulent Flow in Multistage Axial Compressor Blade Row," *Journal of Applied Mechanical*, vol. 2, p. 320–325, 2008.

[16]. S. Peng, X. Zhang, W. Wang, H. Zhang and X. Li, "Numerical Simulation on Unsteady Flow Mechanism of a 1.5-Stage Axial Transonic Compressor," *Journal of Thermal Science*, vol. 33, p. 1851–1866, 2024.

[17]. H. Jia and H. Wu, "Numerical simulation of three-dimensional flow field in transonic compressor rotor.," *Aeronautical and Computational Technology* , vol. 35, p. 3 94–97, 2005.

[18]. F. Wang, L. Zhao, L. He and M. Zhang, " Three-Dimensional CFD Flow Field Analysis and Aerodynamic Optimization of a Multi-Stage Axial Compressor.," *Therm. Turbine* , vol. 41 , p. 215–219, 2012.

[19]. A. Avwunuketa, J. Enyia and S. Oloruntoba, "Numerical and Thermal Finite Element Analysis (FEA) of Idealized Gas Turbine Engine Blade," *International Journal of Aerospace and Mechanical Engineering (IJAME)*, vol. 7, no. 1, pp. 14 - 18, 2020.

[20]. L. Zhang, Y. Liu and S. Sun, "Numerical study on effects of total pressure distortion on unsteady effect of impeller-diffuser interactionin centrifugal compressor.," *Propuls. Technol. 2025, ,* p. 1–14, 2025.

[21]. A. Baretter, B. Godard, P. Joseph, O. Roussette, F. Romanò, R. Barrier and A. Dazin, "Experimental and Numerical Analysis of a Compressor Stage under Flow Distortion," *International Journal of Turbomachinery, Propulsion and Power*, vol. 6, no. 43, pp. 1-12, 2021.

[22]. N. Ma, X. Nan, F. Tang, J. Zhang and R. Liu, "Numerical study on evolution mechanism of inlet total temperature distortion in an axi-centrifugal compressor," *J. Propulsion Technology* , 2024.

[23]. W. Tian, B. Tu and J. Hu, "Numerical Simulation of Influence of Swirl Distortion and Total Pressure Distortion on Performance and Stability of Booster Stage.," *Journal Nav. Aviat. Univ.*, vol. 40, p. 213–227, 2025.

[24]. A. Lesser and R. Niehuis, "Transonic Axial Compressors With Total Pressure Inlet Flow Field

ISSN No:-2456-2165 https://doi.org/10.38124/ijisrt/25dec543

Distortions," in *SME Turbo Expo 2014: Turbine Technical Conference and Exposition*, 2014.

[25]. T. Pan, J. Yan, H. Lu and Q. Li, "Impact of circumferential inlet distortion on different types of stall inceptions in a transonic compressor," *Chinese Journal of Aeronautics*, vol. 37, no. 11, pp. 107-117, 2024.

[26]. G. Zhu, X. Liu, B. Yang and M. Song, "A study of influences of inlet total pressure distortions on clearance flow in an axial compressor," *Journal of Engineering for Gas Turbines and Power*, vol. 143, no. 10, 2021.

[27]. W. Zhang and M. Vahdati, "A parametric study of the effects of inlet distortion on fan aerodynamic stability," *Journal of Turbomachinery*, vol. 141, no. 1, 2019.

[28]. K. Kikuchi, A. Tamura, Y. Matsuo, K. Hirai, H. Kodama and O. Nozaki, " Unsteady three-dimensional analysis of inlet distortion in turbomachinery.," in *Proceedings of the 33rd Joint Propulsion Conference and Exhibit*, Seattle, WA, USA, 1997.

[29]. V. Fidalgo, C. Hall and Y. Colin, "A Study of Fan-Distortion Interaction Within the NASA Rotor 67 Transonic Stage," *Journal of turbomachinery*, vol. 134, no. 5, 2012.

[30]. P. Sun, G. Feng and D. Kui, " Numerical Simulation of the Impact of Total-pressure Distortion on the Aerodynamic Performance of Small-sized Fans.," *Thermal Power Engineering* , vol. 21, p. 259–263, 2006.

[31]. Q. Gao, X. Yang and S. Liu, "Experiment on inlet distortion of high bypass ratio fan and booster," *Journal of Aerospace Power* , vol. 40, p. 44–52, 2025.

[32]. W. Wang, T. He, W. Sun, X. Wang, W. He and B. Wang, "Numerical Investigation of Bleed Rate on Performance of Multistage Axial Compressor.," *Gas Turbine Technol.* , vol. 37, p. 1–10, 2024.

[33]. X. W. Zhang, Y. P. Ju and C. Zhang, " Performance prediction and IGV-stator adjustment optimization of a multi-stage axial-flow compressor.," *J. Eng. Thermophys.* , vol. 41, p. 1418–1427, 2020.

[34]. A. Avwunuketa, B. Bonet, M. Adamu, U. Haruna and O. Fadenipo, "Performance, Characterization and Evaluation of Axial Flow Turbine Engine," *International Journal of Advances in Scientific Research and Engineering (IJASRE)*, vol. 5, no. 10, pp. 124 - 131, 2019.

[35]. R. Steinke, "Design of 9.271-Pressure-Ratio Five-Stage Core Compressor and Overall Performance for First Three Stages," NASA Technical Paper 2597; National Aeronautics and Space Administration , Cleveland, OH, USA, 1986.

[36]. D. Jiang, H. Li, C. Liu, Y. Hu, Y. Li, Y. Yan and C. Zhang, "Aerodynamic Characteristics of Typical Operating Conditions and the Impact of Inlet Flow Non-Uniformity in a Multi-Stage Transonic Axial Compressor," *Processes* , vol. 13, no. 1428, 2025.